

## BONDED ZONE ANALYSIS OF AN ADHESIVE JOINT UNDER SPECIFIC VARIATIONS

M. D. MOHAN GIFT

*Professor, Panimalar Engineering College, Chennai, India*

### ABSTRACT

*Bonded zone analysis in adhesive joints becomes a point of concern when they become exposed to unexpected constraints. The influence of specific parameters like adhesive thickness, composition, and temperature may alter the bonded zone outcomes in the bonded area. Hence, research with a particular focus, like analyzing an adhesive joint subjected to a specific set of variations, needs facilitation. The DCB tests done for the replication of the mode-1 loading characteristics becomes relevant for the analysis. The paper profiles the outcomes of a DCB test done on an adhesive joint between Aluminium and Mild steel substrates subjected to a set of variations, which includes thickness, composition alteration, and test environment temperature. The derived results provide a suitable insight into the influence of the mentioned variations on the bonded zone.*

**KEYWORDS:** Double Cantilever Beam & Corrected Beam Theory

**Received:** Oct 30, 2019; **Accepted:** Nov 19, 2019; **Published:** Feb 04, 2020; **Paper Id.:** IJMPERDFEB202049

### INTRODUCTION

Bonded zone analysis provides insight on the stress involvement whenever dissimilar substrates are bonded adhesively and subjected to different variations. A suitable extent of research is focussed on the beam theory application to decide the area of stress influence in single-lap adhesive joints [1]. Initial analysis done using similar substrates was used for comparative analysis when they replace dissimilar substrates [2]. The research initiative outlined in this paper covers the bonded zone analysis done using adhesive joints bonded between Aluminium and Mild steel substrates. The variations included were adhesive thickness, composition, and temperature.

### LITERATURE REVIEW

The literature reviewed a wide range of papers oriented around the specific variations implemented in this work. The research explicitly studies the influences of thickness, composition, and temperature variations.

The influence of repeated cyclic loading applied on different adhesive layer thickness in DCB experiments was studied by Mall & Ramamurthy [3]. Sela et al. [4] investigated the effects of adhesive thickness under both mode-1 and mode-2 loadings for variations in interlaminar fracture toughness involving CFRP substrates. The fracture of the adhesive layer was analyzed using three variations in thickness by Kafkalidis et al. [5] Some of the literature reiterate the fact that the fracture energy varies with the extent of adhesive thickness as reported in the works of Madhusudhana & Narasimhan [6], Ikeda et al. [7] and Pardo et al. [8]

A similar investigation which made an attempt to relate the stress intensity factors to the bondline thickness range was undertaken by Gleich et al [9]. Mehrabadi [10] in an investigation used a DCB specimen which had a constant adhesive thickness of 0.4mm which was affirmed by placing calibrated steel rods of tolerance

( $0.4 \pm 0.01$  mm) between the GFRP substrates. In another significant investigation, the increment of bond-line thickness from 0.1 to 3 mm attributed to a uniform drop in failure load by Grant et al [11]. The significant works of Taib et al [12] revealed the drop of failure loads which was inversely proportional to the adhesive layer thickness.

Griffiths et al. [13] used the DCB test to measure the fracture energy of a series of cured epoxy resins. Monteiro & D'Almeida [14] analyzed the possibility of mechanical property variation dependence on the hardener-resin proportion variation. Kishore et al. [15] used glass fiber to physically modify the Araldite epoxy resin in an attempt to improve its wear resistance.

The impact of the resin/hardener ratio on the mechanical properties like yield stress and fracture was studied by Pandini et al [16]. The epoxy resin behaviour transitioned between ductile to brittle performance which was dependent on the hardener-resin proportion variation. Another significant investigation which incorporated the infusion of carbon nano-fillers in the epoxy resin resulted in a remarkable increase in the propagation number of the mode-I adhesive fracture energy by M R Gude et al [17]. Suitable development for adhesives to be made for enhanced fracture energy is done by suitable alterations of the chemical stoichiometry by the addition of elastomeric prepolymers which is reported in the patented works of Lutz and Schneider [18].

Adams et al. [19] investigated the strength and state of stress of a dissimilar substrate DCB specimen (Titanium/CFRP substrates) under the impact of the temperature range between  $-500^{\circ}\text{C}$  and  $2000^{\circ}\text{C}$ . Owens and Lee [20] compared the reduction in structural stiffness of another unique substrate DCB specimen (Aluminium/composite substrates) at the selective temperatures of  $-400^{\circ}\text{C}$  and  $230^{\circ}\text{C}$ . Kim et al. [21] investigated the impact of environmental temperature on the fracture behaviour of dissimilar substrates, including thermoplastic polymers and carbon fiber composites in DCB testing. Preliminary research done by the author [22] concentrated on the bonded region of specimens using mild steel similar substrates with the same variations.

The adhesive layer exhibited behaviour transition from brittle to ductile and stick-slip as intermediate for temperatures of  $-50^{\circ}\text{C}$ ,  $22^{\circ}\text{C}$  and  $90^{\circ}\text{C}$  respectively which was promptly reported in the works of Ashcroft et al [23]. The same nature of investigation was extended for mixed mode loading using test environment humidity and temperature as controlling parameters on the crack propagation nature in adhesive joints between aluminium substrates in asymmetric DCB specimens by Datla et al [24]. Walander et al [25] an investigation identified that the Critical Strain Energy Release rate ( $G_{ic}$ ) value was independent of the corresponding temperatures when they were well below the glass transition temperature. However, when the temperature values are in proximity with the glass transition temperatures, there was a pronounced reduction of the  $G_{ic}$  values.

From the reviewed works of literature, it is quite evident that the incorporated variations provide enough insight into the bonded zone nature of the bonded zone in the adhesive joints. But a wide range of researches are not mentioning the influence of variation of the hardener or resin content in the adhesive while creating the specimen. Hence, the present research studies the influence exerted by the mentioned variations on the bonded zone characteristics. Three variations are attempted including the adhesive thickness, composition in the form of hardener resin variation, and temperature.

## EXPERIMENTAL DETAILS

The work analyses a DCB test done on a specimen made of Aluminium and Mild steel substrates bonded with Araldite 2015. The bonded zones are observed based on inducing the variations separately.

- Bond thickness (1, 1.5&2 mm).
- Composition(AS-I, II,& III) given in table(2).
- Temperature ( $T = 30^0\text{ C}$ ,  $50^0\text{ C}$ , and  $70^0\text{ C}$ ).

The following flow chart provides the experimental details.

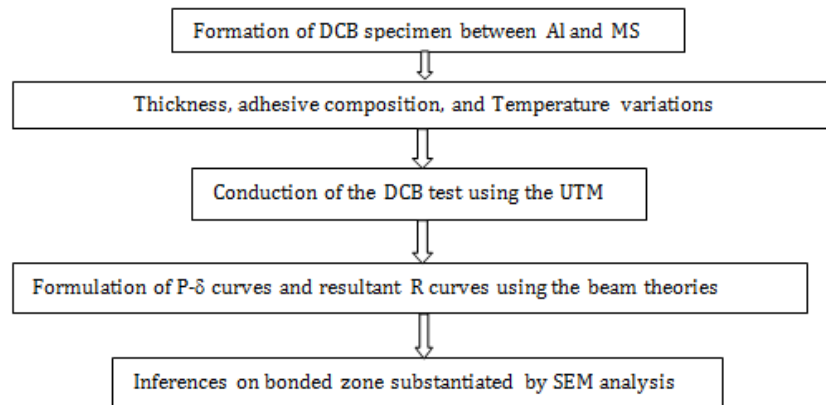


**Figure 1: Experimental Procedure Flow Chart.**

The DCB specimens used mild steel (EN24B) and Aluminium (AA 6061-T6) as substrates. Table 1 lists their material properties. Goyal et al. [26] and Choupani et al. [27] did research similar to the choice of substrate selection and justification in this work. Araldite 2015, being a two-component toughened epoxy adhesive was selected as the adhesive due to its excellent bonding characteristics between the dissimilar substrates.

**Table 1: Substrate Properties**

Sl. No	Substrate	Elastic Modulus(N/mm <sup>2</sup> )	Tensile Strength(N/mm <sup>2</sup> )	Yield Stress(N/mm <sup>2</sup> )	Hardness(HB)
1	AA 6061-T6	$68.9 \times 10^3$	310	276	95
2	EN24 B	$200 \times 10^3$	900	700	250

Figure 2 Shows the Variations Sequence Implemented in the Experiments.

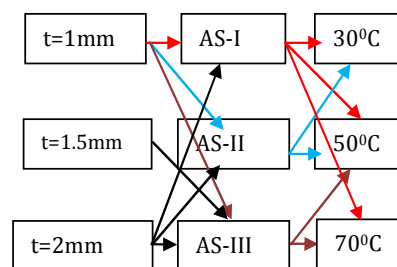


**Figure 2: Variation Combination**

The adhesive thickness is decided based on the substrate thickness before and after joint formation. The thickness( $t$ ) is obtained by subtracting the total joint thickness( $T_j$ ) and twice the substrate thickness using equation(1).

$$t = T_j - 2t_{sub} \quad (1)$$

The resin and hardener are mixed following the proportionality, which led to the formulation of three adhesive

samples(AS-I, II, & III) mentioned in table 2. The hardener volume was fixed, and the resin was varied. Efforts made to keep the resin fixed and the hardener to be varied resulted in complications while trying to incorporate the other variations.

**Table 2: Substrate Properties**

Sl. No.	Proportion Type	Hardener(ml)	Resin(ml)
1	AS-I	5	7
2	AS-II	5	7.5
3	AS-III	5	9

The temperatures selected were based on the glass transition temperature( $T_g$ ) of Araldite 2015, which is  $40^{\circ}\text{C}$ . A muffle furnace was arranged in proximity with the UTM, and the tests were carried out. The deviations in the temperature due to the transfer of the specimens from the furnace to the fixture were systematically recorded. The room temperature specimen was devoid of any arrangements, and the test results were compiled for analysis.

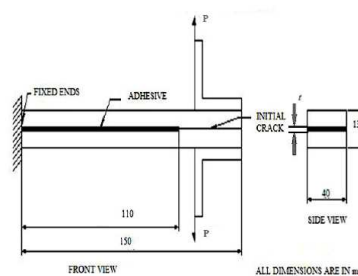


**Figure 3: DCB Specimen Configuration.**

The tests were done by ASTM D 5528-02 on a tensile testing machine having a cross-head displacement range between 0.5 to 5 mm/min, which conforms to ISO 5893. The Corrected Beam Theory (CBT) data reduction scheme shown in the equation(2) was used to obtain the R curve from the P- $\delta$  curves.

$$G_{ic} = \frac{3P\delta}{2b(a+|\Delta|)} \quad (2)$$

Here  $|\Delta|$  denoted a correction parameter derived from the plot generation between the compliance cube-root( $C^{1/3}$ ) and the bonded zone length(a).

## OBSERVED SEPARATION NATURE

The three variations imposed during the DCB test were independently done on the Aluminium mild steel substrate specimen to study the bonded zone nature during each test. Table 3 broadly lists the nature of separation when the variations were implemented. Figures 4 and 5 reveal the AA 6061-T6 and EN 24 B specimens before the bonding was initiated. Figures 6 and 7 reveal the DCB specimen and the ASTM Standard followed for the specimen formation.

**Table 3: Observed Separation Nature**

Variations Imposed	Sub-Variations	Fixed Variation	Observed Separation Nature
Thickness	t=1mm	AS-I, T = $30^{\circ}\text{C}$	Erratic
	T = 1.5mm		Non-uniform resistance and sudden
	T = 2mm		Massive initial resistance followed by abrupt bonded zone more pronounced than that for t=1.5mm
Composition	AS-I	t= 1mm, T = $30^{\circ}\text{C}$	Uniform
	AS-II		Non-uniform resistance and sudden
	AS-III		Heavy resistance and abrupt

Temperature	$T = 30^{\circ}\text{C}$	AS-I, $t = 1\text{mm}$	Zig-zag
	$T = 50^{\circ}\text{C}$		Rapid separation
	$T = 70^{\circ}\text{C}$		Bonded zone more pronounced than that for $T = 50^{\circ}\text{C}$



Figure 4: Aluminium Substrates Before Bonding.



Figure 5: Mild-Steel Substrates.



Figure 6: Fabricated DCB Specimen.

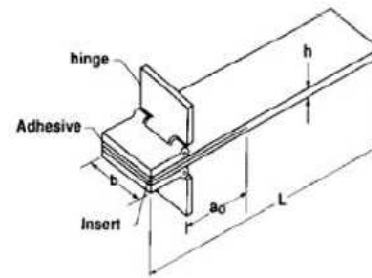


Figure 7: DCB Specimen (ASTM D 5528-02).

## RESULTS AND DISCUSSIONS

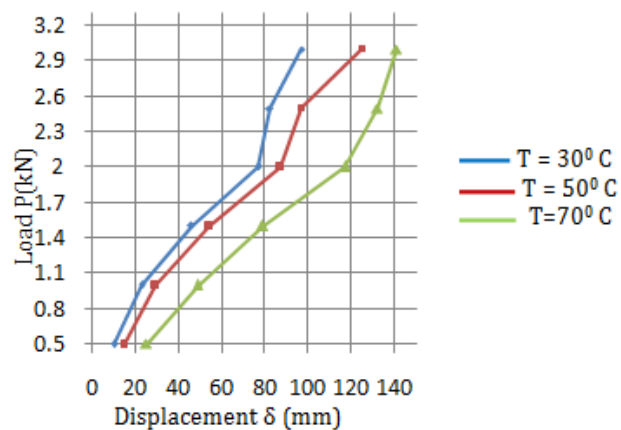


Figure 8: P- $\delta$  Curve for Temperature Variation (AS-I,  $t = 1\text{mm}$ ).

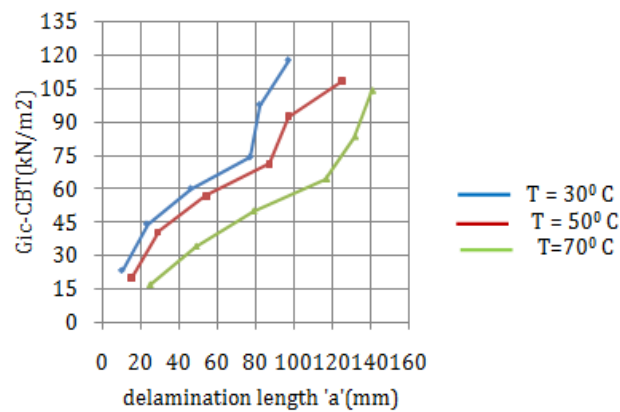


Figure 9: R Curve using CBT.

The figures 8 and 9 represented the  $P-\delta$  curve and the resultant R curve obtained using the CBT for the specimen which used the AS-II adhesive and a thickness of 1mm. The  $P-\delta$  curve and the R curve revealed the bonded zone nature of the AS-I adhesive under temperature variations. After 2 kN, the linearity abruptly ended for all three temperatures, which are characteristic of the bonded zone nature mentioned in the table 3 for the AS-I, 1mm thickness combination. The proportional equality of the resin and hardener contributed to the bonded zone behavior mentioned in the previous statement.

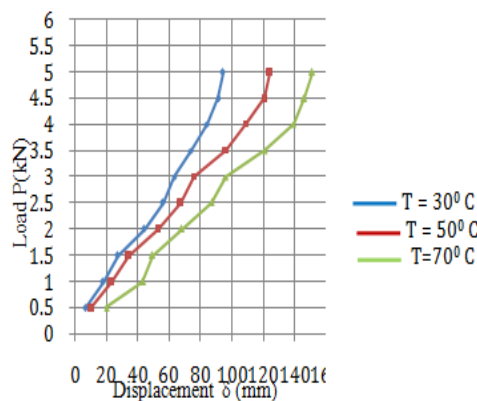


Figure 10:  $P-\delta$  Curve for Temperature Variation (AS-II,  $t=1\text{mm}$ ).

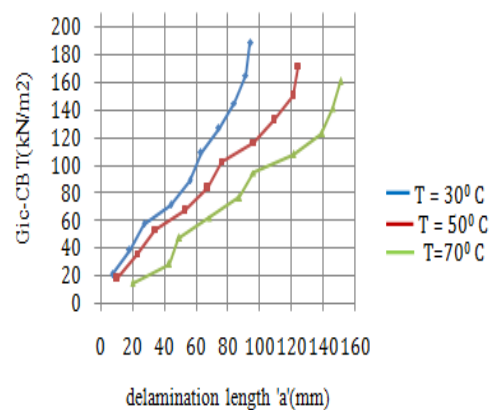


Figure 11: R Curve using CBT.

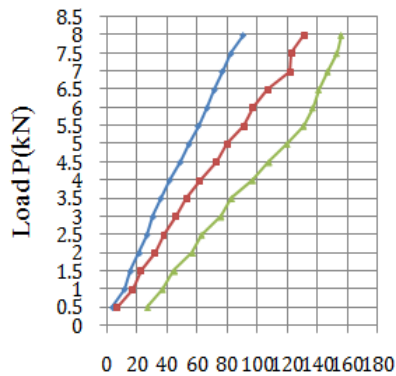


Figure 12:  $P-\delta$  Curve for Temperature Variation (AS-II,  $t=1\text{mm}$ ).

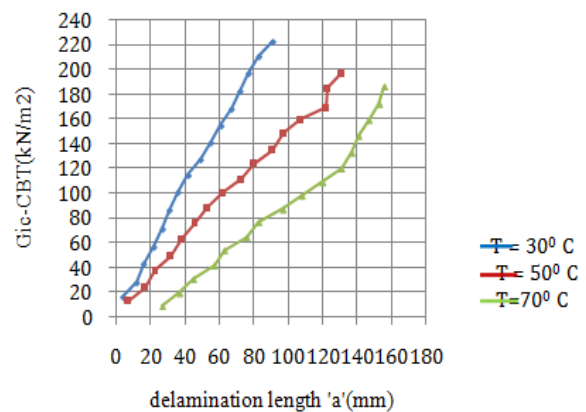
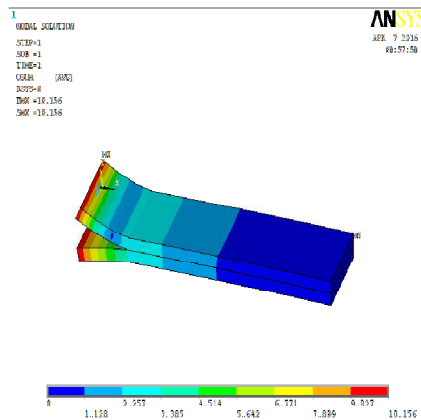


Figure 13: R curve using CBT.

The plots revealed in figures 8-13 substantiated the bonded zone separation mentioned in table 2. They represent the P- $\delta$  curves and the resultant R curves obtained from the DCB tests done on specimens using the AS-I, II, & III adhesive types and 1mm bond thickness subjected to the three temperature variations following the sequential test pattern mentioned in figure 2. The AS-II adhesive used under elevated temperatures induced marginal linear variations visible in both the P- $\delta$  and the R curve. The variations indicated the inconsistency mentioned in table 2. The R curve also highlights a degree of necking at the fourth value for all the three temperatures. The plots reveal the degree of resistance lowering to the separation which is accrued due to the increase in the temperature from 30<sup>0</sup> C to 70<sup>0</sup>C. Under increased temperature the lowering of resistance to separation was characterised by acute degree of necking in the R curve shown in the figure 9.

## STRUCTURAL ANALYSIS

A structural analysis was initiated for the DCB specimens when the adhesive thickness was kept as 1 mm and 1.5mm. The following diagrams (Figures 14 and 15) reveal the stress distribution plots for the thickness of 1mm and 1.5 mm.



**Figure 14: Stress Distribution Plot-1mm Thickness.**

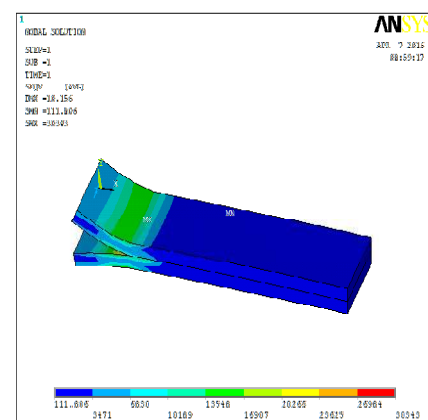


**Figure 15: Stress Distribution Plot-1.5 mm Thickness.**

The Figure 14 reveals the stress distribution contours in the DCB specimen incorporating the thickness variation of  $t = 1\text{mm}$ . The maximum stress areas are seen as distributed near the delamination tip zone and on the top substrate zone. The maximum stress value is seen as  $0.027825\text{ N/mm}^2$ . The stress contours are seen as gradually receding towards the specimen tip in a non-uniform manner. The recession is also seen towards the other end of the specimen and then levels out as a constant value.

For a thickness variation of  $t = 1.5\text{mm}$ , a 3D stress distribution plot is obtained in the figure 15 which shows a maximum stress value of  $30.35\text{ kN/mm}^2$ . The maximum stresses are more concentrated in the delamination tip zone as well as in the substrate zones directly above and below. The recession in the stress value is seen in a gradual manner towards the crack tip. Furthermore, the recession is abrupt in the other direction.



## SEM ANALYSIS

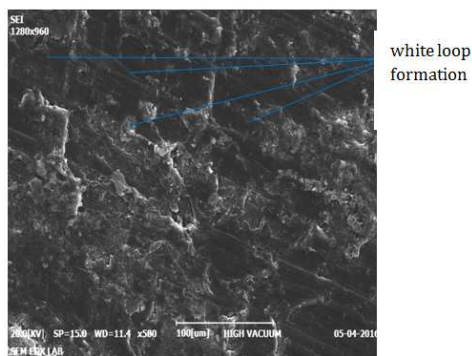


Figure 16: SEM Image of AS-I(100x).

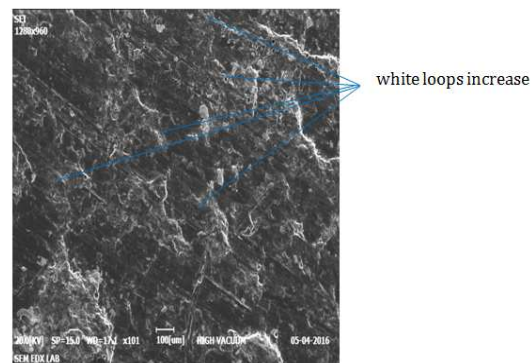


Figure 17: SEM Image of AS-II(100x).

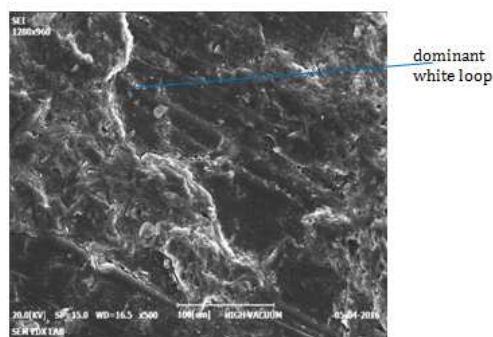


Figure 18: SEM Image of AS-III(100x)

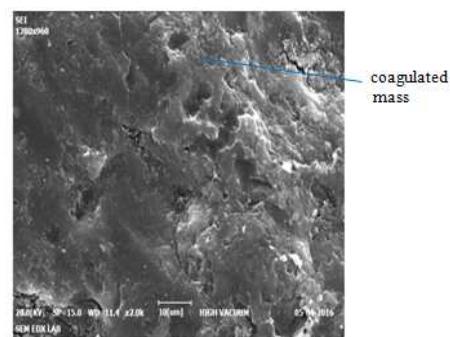


Figure 19: SEM Image of AS-I(500x)

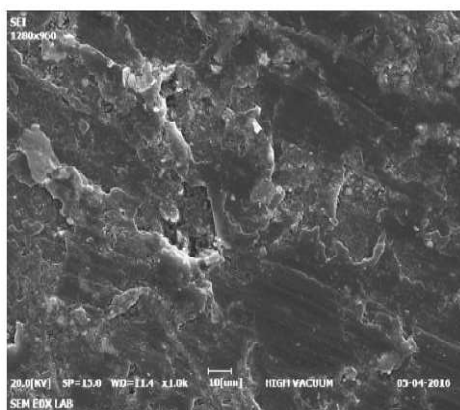


Figure 20: SEM Image of AS-II(100x).

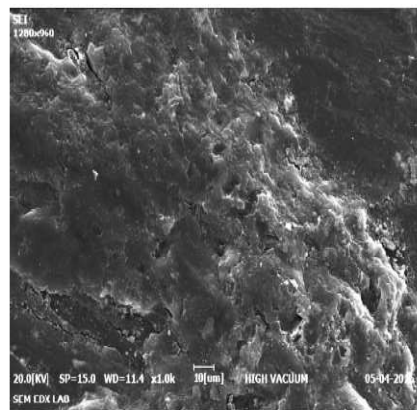


Figure 21: SEM Image of AS-III(500x).

The SEM image of the AS-1 bonded zone shown in figure.16 revealed the bonded zone tip towards the end of the separation sequence. The white loop, like arrangement dispersed throughout the entire image, represents the prominent characteristic that represents the resin content in the composition. Figure 17 shows another SEM image of the AS-II bonded zone also taken at the end of the separation sequence like AS-I. The arrangement of the white loops seems to be more prominent which justifies the increase in the resin content. Figure 18 represents the AS-III bonded zone, revealing the white loop region extending from the top left towards the bottom right in the form of an irregular curved line. The prominence of the white loop like regions are characteristic of the responses to the resin content variation which



significantly influences the separation characteristics and agrees with table 2 and the plots.

The pattern in Figure 18 is prominently visible in an incomplete loop form. The remaining regions show slightly inclined parallel line patterns extending from the top left region to the bottom right regions of the SEM image. The patterns and wavy dispersed forms are considered to be indicative parameters regarding the hardener resin proportion equivalence which has a pronounced effect on the separation retardation sequences observed when dissimilar substrates are subjected to mode-I loading in the DCB tests.

The top right and the bottom left regions show more dispersion of the white stripes in a random manner whereas the white regions are more concentrated in the form of granules in the middle region of the SEM image. The remaining regions are seen as marginally inclined and parallel line patterns. This is an indicative parameter highlighting the dispersion of the resin component. The white region is seen extending from the top left region and extending towards the bottom right region in the form of an irregular curved line. The remaining portions of the SEM image reveal the white regions as dispersed and clustered granule form more concentrated in the right border.

The Figure 19 shows the adhesive layer composed of the AS-I adhesive seen at a magnification of 500x. The white regions are seen as a coagulated mass more pronounced on the top right corner of the image. The rest of the image is composed of a uniform dispersed mass sprinkled with black cavities at different locations. A non-uniform line is seen as propagating from the top towards the bottom of the image. It may be noted as significant that the two distinct patterns of coagulated white regions and the uniform dispersed mass cluttered with black cavities occupy an almost equal space in the image which is due to the equivalence of hardener-resin proportion.

The Figure 20 reveals the SEM image taken at 500x magnification of the bonded zone of the AS-II adhesive. Unlike the previous images, the white regions are dispersed throughout the region as wavy patterns among inclined and parallel line patterns. The white wavy patterns are more concentrated in the middle region of the fractograph. The middle region of the SEM image shows a distinct cavity which is seen as a black zone contrasting with the rest of the white wavy patterns. This is due to the non-uniformity in the resin distribution.

The Figure 21 reveals the image taken with a higher degree of resolution and magnification of the adhesive layer constituting the AS-III adhesive. The patterns highlighted in the previous image (Figure 13) of the same proportions are further enhanced in the present image which reveals the white pattern as a dispersed and coagulated solid mass dominating the entire region which is indicative of the hardener dominance. The black regions are more clustered in the top right region of the image. The line patterns in the other fractographs are not visible which is due to the dominating influence of the white region as a dispersed and coagulated solid mass mentioned previously. The consistency of the solid mass is more in the bottom right corner of the image which gets reduced in intensity in the remaining parts.

## CONCLUSIONS

The process of procuring the P- $\delta$  curve and the R curve and the SEM images assist in understanding the nature of the adhesive-bonded zone under the imposed variations.

- An increase in the resin proportion produces an elevation of the  $G_{ic}$  value as shown from the values obtained for AS-II which are slightly less when compared with AS-I and III.
- The presence of dissimilar substrates and the variation in the hardener-resin proportion affected the  $G_{ic}$  values

during bonded zone.

- The AS-III formed DCB specimen revealed uniform variations among the results obtained from the CBT and SEM results. The variations were slightly contrasting to the AS-II, and AS-I formed DCB specimens.
- Similarly, the elevation of temperature from 30<sup>0</sup>C to 50<sup>0</sup>C and subsequently to 70<sup>0</sup>C saw some coincidence in the establishment of several basic white loop patterns that were significantly visible from the SEM images.
- The specimen that had an AS-II adhesive under an adhesive layer thickness of 1mm and a temperature of 50<sup>0</sup> C produced outstanding results, which were found to be suitable for excellent bonded zone characteristics.
- The investigation was able to successfully determine the optimal configuration of parameters such as dissimilar substrate combination, suitable hardener-resin proportion variation in the form of AS-I, II, and III, test temperatures, and thickness of the adhesive layer for minimal delamination in the adhesive joint.

Hence the work which focused on the influences of the adhesive thickness composition and temperature variations was done to study the bonded zone sequences of a dissimilar substrate formed DCB specimen. The generated results provided reasonable insight into the bonded zone nature of the adhesive joint.

#### REFERENCES

1. Wu, Z, Romeijn, A & Wardenier, J 1997, 'Stress expressions of single-lap adhesive joints of dissimilar adherends,' *Composite Structures*, vol. 38, no. 1-4, pp. 273-280.
2. Spelt, JK, Azari, S & Papini, M 2011, 'Effect of adhesive thickness on fatigue and fracture of toughened epoxy joints—part I: experiments,' *Engineering Fracture Mechanics*, vol. 78, no. 1, pp. 153-162.
3. Mall, S & Ramamurthy, G 1989, 'Effect of bond thickness on fracture and fatigue strength of adhesively bonded composite joints,' *International Journal of Adhesion & Adhesives*, vol. 9, no. 1, pp. 33-37.
4. Sela, N, Ishai, O & Sills, LB 1989, 'The effect of adhesive thickness on interlaminar fracture toughness of interleaved CFRP specimens,' *Composites*, vol. 20, no. 3, pp. 257-264.
5. Kafkalidis, MS, Thouless, MD, Yang, QD & Ward, SM 2000, 'Deformation and fracture of adhesive layers constrained by plastically-deforming adherents,' *Journal of Adhesion Science and Technology*, vol. 14, pp. 1593-1607.
6. Madhusudhana, KS & Narasimhan, R 2002, 'Experimental and numerical investigations of mixed-mode crack growth resistance of a ductile adhesive joint,' *Engineering Fracture Mechanics*, vol. 69, pp. 865-883.
7. Ikeda, T, Yamashita, A, Lee, D & Miyazaki, N 2000, 'Failure of a ductile adhesive layer constrained by hard adherents', *Journal of Engineering Materials and Technology*, vol. 122, pp. 80-85.
8. Varaprasad, S. P., & Rao, R. P. *Design and Analysis of A Multi Layer Substrate Single Patch Microstrip Patch Antenna for Enhancing the Beam Width with Control on Directivity*.
9. Pardoen, T, Ferracin, T, Landis, CM & Delannay, F 2005, 'Constraint effects in adhesive joint fracture,' *Journal of the Mechanics and Physics of Solids*, vol. 53, pp. 1951-1983.
10. Gleich, DM, Van Tooren, MJL, Beukers, A, 2001, 'A stress singularity approach to failure initiation in a bonded joint with varying bondline thickness', *Journal of Adhesion Science & Technology*, vol 15(10), pp.1247-1259.
11. Mehrabadi, S, A, 2011, 'Experimental and Numerical Failure Analysis of Adhesive Composite Joints', *International Journal of Aerospace Engineering*, vol 2012, pp.1-6.

12. Grant, LDR, Adams, RD, DaSilva, LFM, 2009, 'Experimental and numerical analysis of single lap joints for the automotive industry', *International Journal of Adhesion & Adhesives*, vol.29, pp.405-413.
13. Taib, AA, Boukhili, R, Achiou, S, Gordon, S, Boukehili, H, 2006 'Bonded joints with composite adherends. Part 1. Effect of specimen configuration, adhesive thickness, spew fillet and adherend stiffness on fracture', *International Journal of Adhesion & Adhesives*, vol. 26, pp.226-236.
14. Griffiths, R & Holloway, DG 1970, 'The fracture energy of some Epoxy resin materials,' *Journal of Material Science*, vol. 5, pp. 302-307.
15. Monteiro, SN & D'Almeida 1997, 'The role of the Resin Matrix/Hardener ratio on the Mechanical properties of low volume fraction epoxy composites,' *Advanced Performance Materials*, vol. 4, no. 3, pp. 285-295.
16. Kishore, Sampathkumaran, P, Seetharamu, S, Vynatheya, S, Murali, S & Kumar, RK 2000, 'SEM observations of the effects of velocity and load on the sliding wear characteristics of glass fabric-epoxy composites with different fillers,' *Wear*, vol. 237, pp. 20-27.
18. Pandini, S, Baldi, F, De Santis, R, Bignotti, F, 2008 'Epoxy /Layered-Silicate Nanocomposites: Effect of The Matrix Composition On large Deformation and Fracture Behavior', 4th International Conference Nanofun-poly Rome (Italy), April 16 - 18, 2008.
19. Gude, MR, Siliva GP, Urena A, 2015, 'Toughening effect of carbon nanotubes and carbon nanofibres in epoxy adhesives for joining carbon fibre laminates', *International Journal of Adhesion and Adhesives*, vol 62, pp.139-145.
20. Agarana, M. C., & Agboola, O. O. (2015). ANALYSIS OF TORSIONAL RIGIDITY OF CIRCULAR BEAMS WITH DIFFERENT ENGINEERING MATERIALS SUBJECTED TO ST. VENANT TORSION. *International Journal of Research in Engineering & Technology (IMPACT: IJRET)*, 3(2), 33-46.
21. Lutz A, Schneider D, 2006, 'Toughened epoxy adhesive composition', Applicaton #: 20060276601 - Class: 525528000 (United States Patent and Trademark Office), Dow Chemical Company - Midland, Michigan, United States of America.
22. Adams, RD, Coppedale, J & Mallick, V 1992, 'The effect of temperature on the strength of adhesive joints,' *International Journal of Adhesion and Adhesives*, vol. 12, no. 3, pp. 185-90.
23. Owens, JFP & Lee-Sullivan, P 2000, 'Stiffness behavior due to fracture in adhesively bonded composite to Aluminium joints - Experimental,' *International Journal of Adhesion and Adhesives*, vol. 20, no. 1, pp. 47-58.
24. Kim, Young-Ki, Ye, Lin, Yan & Chen 2005, 'Fracture behavior of polyetherimide (PEI) and interlaminar fracture of CF/PEI laminates at elevated temperatures,' *Polymer Composites*, vol. 26, no. 1, pp. 20-28.
25. Alexis SJ, Kumar PS, & Gift MDM 2015, 'Determination of decisive parameters in the crack propagation analysis of an adhesive joint,' *Indian Journal of Science and Technology*, vol.8, pp.35-39.
26. Ashcroft, I, A, Hughes, D, J, Shaw, S, J, 2001, 'Mode I fracture of epoxy bonded composites joints: 1. Quasi-static loading', *International Journal of Adhesion and Adhesives*, vol 21, pp.87-99.
27. Datla NV, Papini M, Ulciny J & Spelt, JK, 2011 'The effects of test temperature and humidity on the mixed-mode fatigue behavior of a toughened adhesive aluminum joint', *Engineering Fracture Mechanics*, vol.78(6), pp.1125-1139.
28. Ahmed, A. K. I. L. (2014). Post buckling analysis of sandwich beams with functionally graded faces using a consistent higher order theory. *Int. J. Civil, Struct. Envir*, 4(2), 59-64.
29. Walander T, Biel A & Stigh, U 2013 'Temperature dependence of cohesive laws for an epoxy adhesive in mode I and mode II

- loading'.. *International Journal of Fracture*, vol.183, pp.203-221.
30. Goyal, VK, Johnson, ER, Goyal & Vi, K 2008, 'Predictive strength fracture model for composite bonded joints,' *Composite Structures*, vol. 82, no. 3, pp. 434-446.
31. Choupani, N 2008, 'Mixed mode cohesive fracture of Adhesive joints: Experimental and numerical studies,' *Engineering Fracture Mechanics*, vol. 75, no. 15, pp. 4363-4382.

## AUTHOR PROFILE



**Dr.M.D.Mohan Gift** is a Professor in the department of Mechanical Engineering, Panimalar Engineering College, Chennai. He did his BE Mechanical in the year 1997 at Madurai Kamaraj University and his ME in Engineering Design in the year 2000 from the Bharathiyar University. He did his research which was focussed on delamination analysis in an Adhesive joint between dissimilar substrates. He got his doctorate in the year 2017 from the Anna University. He has a wide range of teaching experience of about 20 years. He has worked in prestigious Universities like Karunya University. He has authored several publications of international repute.

## Publications 12